

Model Predictive Control Based Grid Connected Inverter for Renewable Energy Applications

K.Balakrishnan¹, K.Yasoda²

¹Department of Electrical and Electronics Engineering, Government College of Technology, Coimbatore-641013, India

E-mail: ¹balakrishnansuryaprakash@gmail.com, ²yasoda@gct.ac.in

Abstract

Model Predictive Control (MPC) for grid-connected inverters has been presented in this paper. The standard proportional-integral controller based system is replaced by this control method for a two-level inverter using Euler's approximation technique to improve the inverter's dynamic response. To anticipate the grid-connected inverter's longer-term behaviour, a replacement predictive mathematical model is offered, which is likened to the reference signal to decide the system's cost function. With this MPC approach, the cost functions of the converter are derived using all possible switching vectors. The associated switching vector for the minimal possible function is then chosen to activate the inverter switches throughout the subsequent sampling instant. The suggested scheme is validated in Simulink to verify its effectiveness and performance. In comparison to the PI-based controller, total harmonic distortion (THD) and current error are minimized.

Keywords: Model Predictive Control, Total harmonic distortion

1. Introduction

As energy from renewable sources has risen in importance, more distributed energy units are being used and tied to local power systems via power converters, such as PV panels, wind turbines etc. These DGs are assimilated to a common AC or DC bus with energy storage systems (ESS) to frame a microgrid in to get more capacity and control adaptability to meet system stability and power quality standards. Grid supporting capacity is another promising capability of DG systems. Because of varying load demand, power system stabilization has been a difficult research task in past few decades. In this sense, the DGs can

be configured to provide active and reactive power compensation, and thus to provide active and reactive power compensation.

In this context, the DGs can be controlled to provide active and reactive power compensation, thereby supporting the voltage and frequency adjustment of the main power system. As a result, power converters must operate more efficiently and effectively in order to ensure high power quality and dynamic stability. There are several existing control strategies for grid-connected inverters, with direct power control (DPC) being one of the most popular.

Model based control has recently emerged as an appealing substitute for power converter management due to its flexible control scheme that allows for the easy integration of system limitations. The model of the system is utilized in this control to forecast system behaviour based on current states and control actions, and a cost function is then used as a criterion to identify the best switching states. However, there is relatively little information in the literature regarding MPC-based variable power regulation for grid-connected inverters. In reality, flexible power regulation is crucial for DGs since, as previously stated, following grid connection, frequency regulation via active power management and voltage support via reactive power compensation are required. This paper proposes a model-predictive direct power regulation technique for grid-connected inverters in PV systems that takes use of the flexibility of the MPC approach. To decrease power ripples, a cost function is first defined. Then, to compensate for the one-step delay in digital implementation, a model-based system is designed. Furthermore, another standard is familiarized into the cost function to minimize the frequency of switching in order to reduce inverter switching loss and thus boost power conversion efficiency. The simulation and experimental data both support the hypothesis.

2. Proposed Work

In this proposed work, two complex load current references are displayed for the duration of the reference. Currents at $i^p(k + 1)$ are computed by numerical computation and using the numerical value of measured current and all the possible voltages. Consider the voltage V_2 which represents the anticipated current that is nearest to the expected value, as depicted in Figure 1. But $i^p_\alpha(V_{0,7})$ refers to the expected current if the voltage V_0 or V_7 is applied at time k . Vector V_2 and V_6 minimize the error in current I_α , while vectors V_2 and V_3 in the current I_β . The value of cost function is directly related to the inaccuracy as shown in table 1. For present control, viewing these errors and distances is simple, but for more

sophisticated cost functions, these charts become difficult or impossible to construct. The selection of voltage vector which is related to the minimum current error is computed numerically as shown in Figure 2. The voltage vector V_2 causes the minimum error in this case. After that, the voltage V_2 is chosen and applied to the inverter.

2.1 Working Principle

The process of discretization of the current flow through the load for a sample time is described in this section. From observed current and voltage at the present sampling point k , the model is utilized to estimate the load current at the next interval. Several discretization approaches can be utilized to create a discrete-time model that can be used to make predictions. The discrete-time model can be derived by a straightforward approximation of the derivative if the load can be treated as a first-order system. The system with high complication, this technique may lead to flaws into the system, necessitating the use of a more precise discretization process.

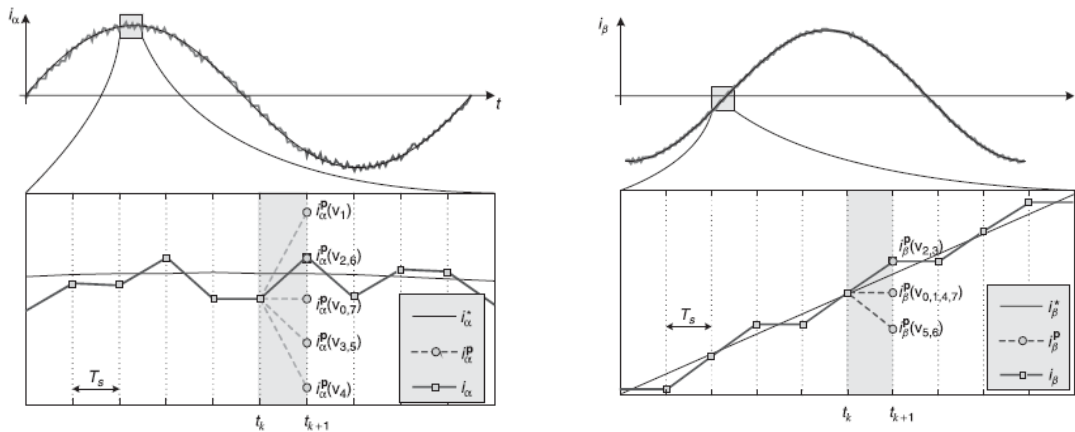


Figure 1. Reference and predicted currents

Table 1. Cost function

Voltage vector	Cost function
V_0, V_7	$c_{0,7} = 0.6$
V_1	$c_1 = 0.892$
V_2	$c_2 = 0.24$
V_3	$c_3 = 0.42$
V_4	$c_4 = 0.96$
V_5	$c_5 = 1.24$
V_6	$c_6 = 1.19$

The derivative of the load current is replaced with a forward Euler's technique. That is, the derivative $\frac{di}{dt} = \frac{i(k+1)-i(k)}{T_s}$ is substituted in voltage equation forecast the load current for different voltages.

In this way, the estimated current is being related at each sampling interval and then the minimum numerical value of cost function is selected, and hence the switching vector related to the minimum error is selected.

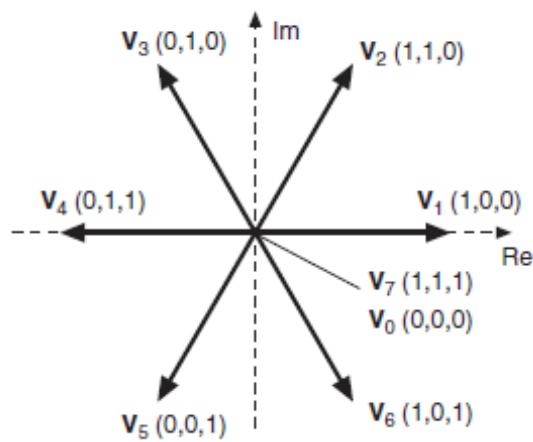


Figure 2. Voltage vectors with their switching combinations.

2.2 Flow diagram

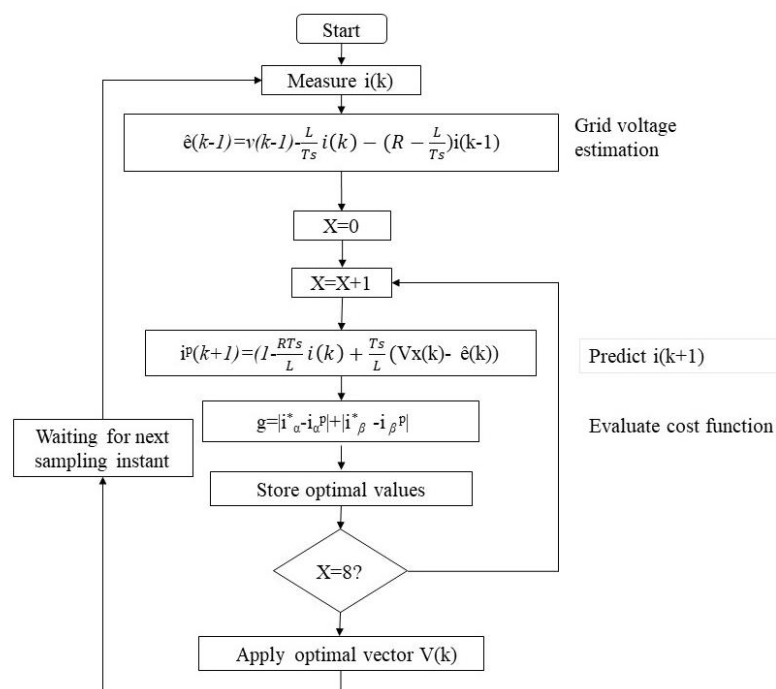


Figure 3. Flow diagram

Figure 3 depicts the system's flow diagram. In which the first step is to find $i(k)$ and then using $i(k)$, the instantaneous value of grid voltage is estimated. By using the grid voltage, $i(k+1)$ is computed. Then cost function is evaluated to switch on the power electronics switch to reduce the error. This is how this algorithm works at each sampling instant.

2.3 System modeling

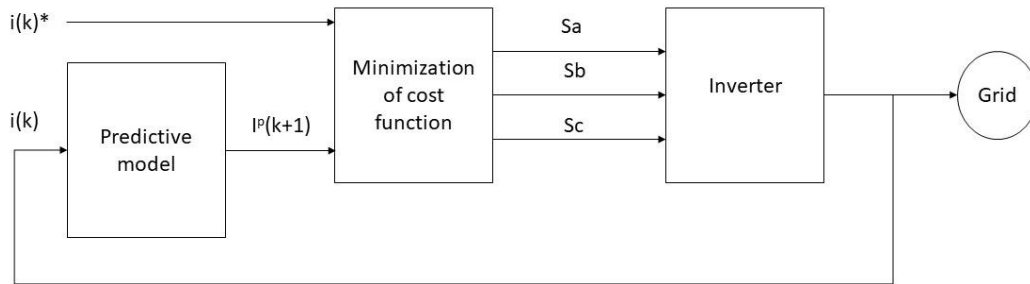


Figure 4. Block diagram

As show in figure 4, the overall system consists of an inverter and associated control block with grid.

2.4 Converter Model

The three-phase inverter's power circuit diagram is represented in Figure 5. The switching states S_q with $q=1,2,\dots, 6$, are mentioned below:

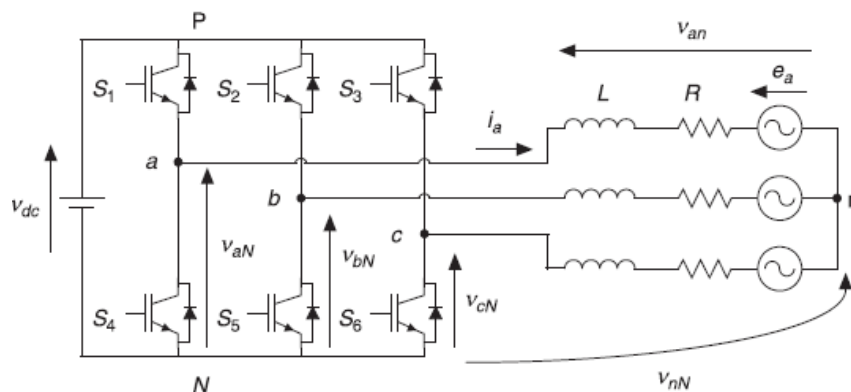


Figure 5. Voltage source inverter power circuit

This switching combination defines the value of the output voltages,

$$V_{aN} = S_a V_{dc}, \quad V_{bN} = S_b V_{dc}, \quad V_{cN} = S_c V_{dc}$$

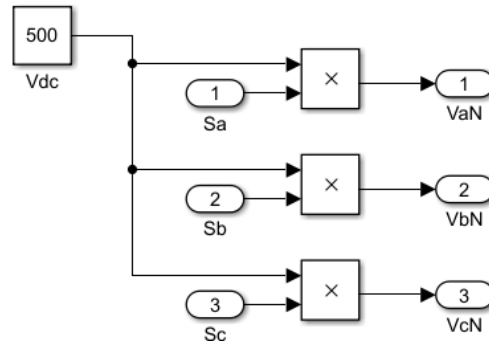


Figure 6. Inverter simulink model

Considering the vector $a = e^{j2\pi/3}$, which signifies the 120° phase angle between the phases. The voltage vector can be defined as

$$v = \frac{2}{3}(V_{aN} + aV_{bN} + a^2V_{cN}) \quad (1)$$

where ,

v_{aN} is the phase voltage of the inverter. Similarly, all the voltages for each possible switching sequence are computed.

2.5 Modeling of Grid

Taking into account the definitions of variables from the circuit shown above, the equations for load current dynamics for each phase can be written as

$$V_{aN} = L \frac{di_a}{dt} + Ri_a + V_{nN} + e_a \quad (2)$$

$$V_{bN} = L \frac{di_b}{dt} + Ri_b + V_{nN} + e_b \quad (3)$$

$$V_{cN} = L \frac{di_c}{dt} + Ri_c + V_{nN} + e_c \quad (4)$$

Where,

R and L are line resistance and inductance respectively.

The voltage equation can be computed as follow,

$$V = L \frac{d}{dt} \left(\frac{2}{3} (i_a + ai_b + a^2i_c) \right) + R \left(\left(\frac{2}{3} (i_a + ai_b + a^2i_c) \right) \right) + \left(\frac{2}{3} (e_a + ae_b + a^2e_c) \right) + \left(\frac{2}{3} (V_{nN} + aV_{nN} + a^2V_{nN}) \right) \quad (5)$$

The grid voltage and load currents are estimated by using the following expressions.

$$i = \frac{2}{3} (i_a + ai_b + a^2i_c) \quad (6)$$

$$e = \frac{2}{3}(e_a + ae_b + a^2e_c) \tag{7}$$

Then the load current dynamics can be described by the vector differential equation

$$V = Ri + L \frac{di}{dt} + e \tag{8}$$

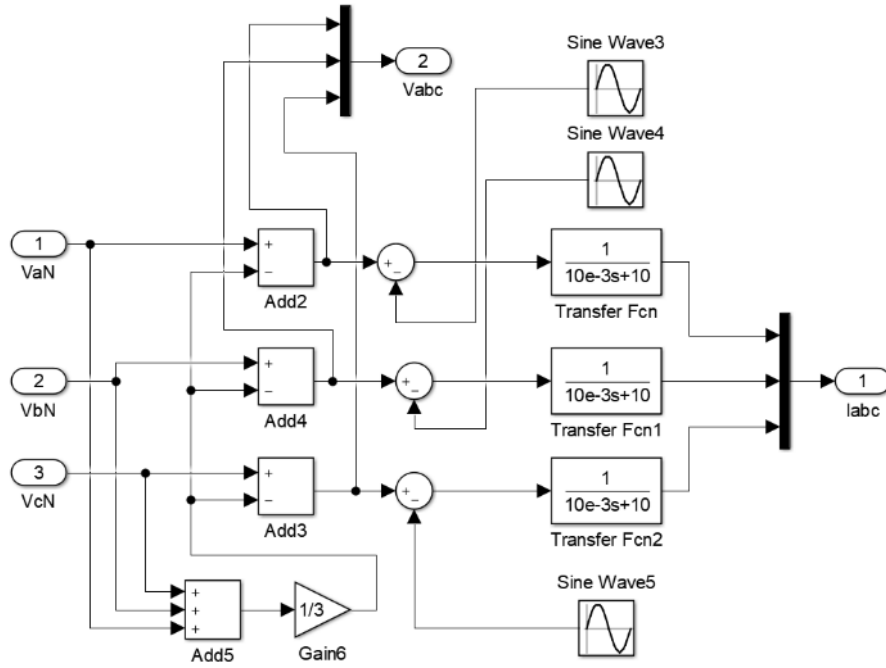


Figure 7. Grid model

3. Results and Discussion

The system parameters considered for simulation is tabulated as shown in table 2.

Table 2. System parameters

Resistance	R	10
Inductance	L	10mH
Grid voltage	V	100V (p-p)
Frequency	f	50Hz
DC source voltage	V _{dc}	500V
Sampling period	T _s	10 and 25 ms

The simulation model consists of five important elements such as references, coordinate conversion, control algorithm, model of inverter and the grid.

An embedded MATLAB function block was used to create the prediction method. At the sample time defined for the prediction algorithm, this block must be configured to use a discrete updating mechanism. This may be done quickly with the Simulink model explorer, which also allows the algorithm's variables to be defined as inputs, outputs, or parameters.

The control function is declared in the code, with the gating signals as outputs. The reference and the measured value of current both stated in two-phase coordinates are the algorithm's inputs.

By applying the Laplace transform,

$$I_a \text{ is calculate by } \frac{I_a}{V_{an}-E_a} = \frac{1}{Ls+R} \text{ and similarly for other phases.}$$

The uppercase variables in the time domain reflect the appropriate lower case variables' Laplace transformations. The load current is the output of the grid model using line parameters, and the voltage derived by subtracting the instantaneous value of grid voltage from the equivalent load voltage is the input. To recreate the grid voltage, which is assumed to be sinusoidal in shape with constant amplitude, standard sine wave blocks are employed.

For this algorithm to operate, the ideal vector chosen by the technique and the instantaneous value of measured current must both be retained from the previous sampling instant. These values are used to evaluate the load back-emf, to establish and configure these persistent variables, and to estimate the grid voltage.

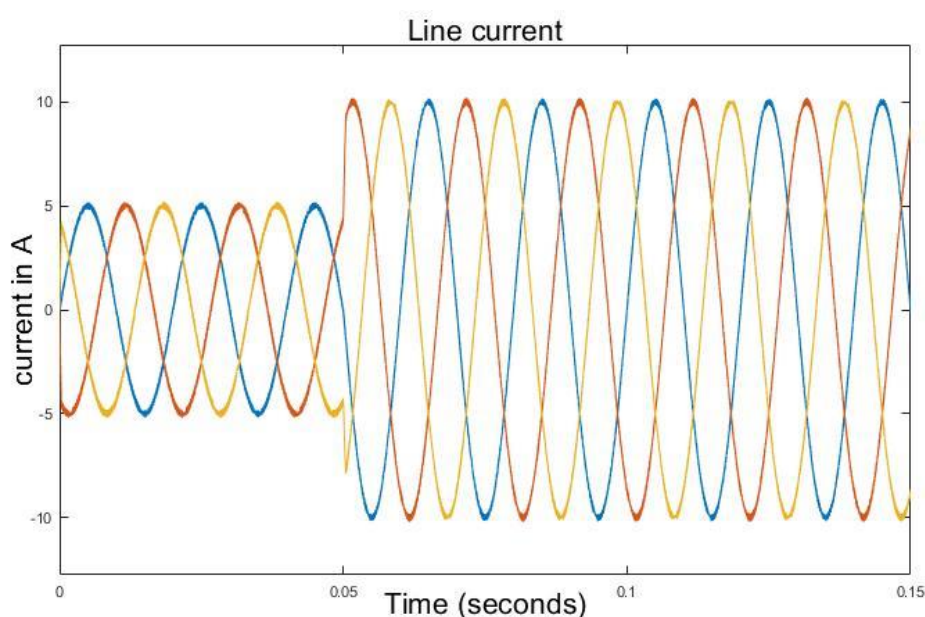


Figure 8. Line current spectrum in steady state

Transient evaluations using the MPC approach, as shown in Figure 8, are performed to demonstrate the resilience of the control schemes. In addition, a step reference is given, with the results displayed in Figure 8, where the amplitude of the step reference is 5 A during the time period 0.0 to 0.05 S, and increases to 10 A at the time instant of 0.05 S. The findings reveal that the predictive current replicates the reference current without delay, although it performs better in terms of benchmark deviation than the reference current.

Accurate current control is possible in this control with minimum error and better transient response as shown in figure 8. Since the response time is minimum, power flow is smooth in nature.

Line current ($T_s=10e-6$ S)

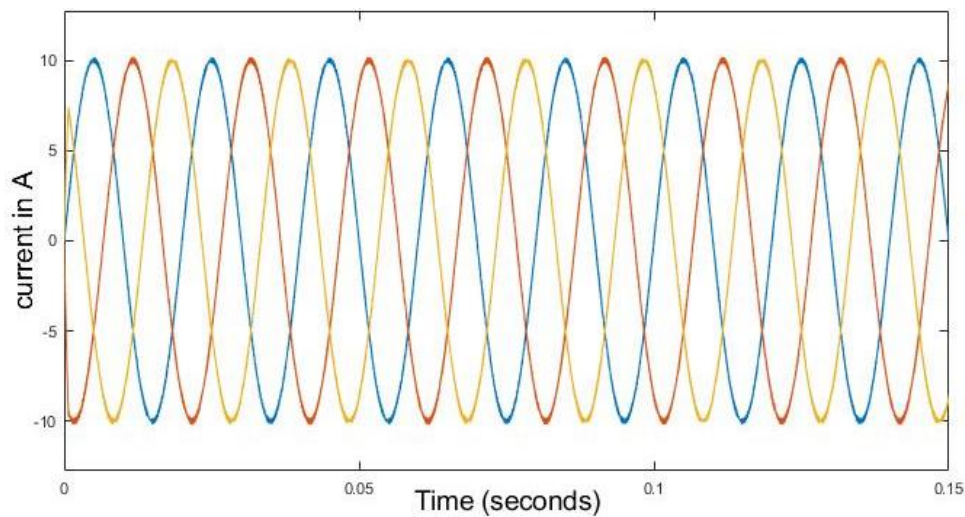


Figure 9. Line current at $T_s=10e-6$ S

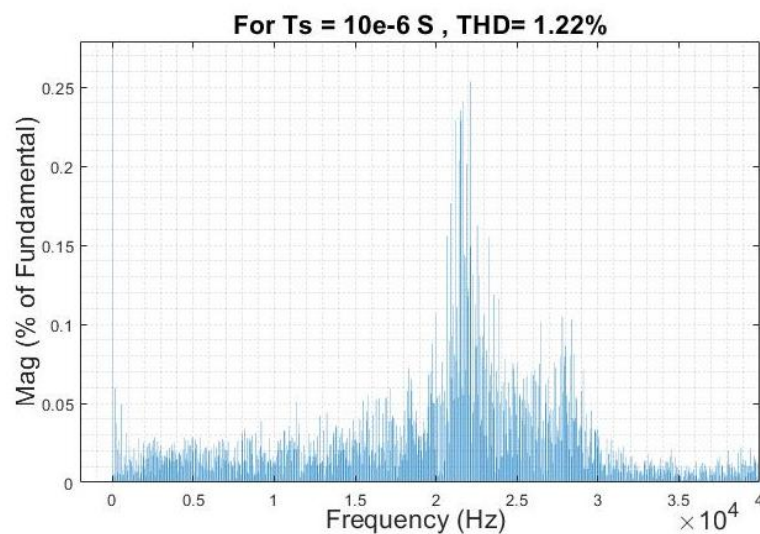


Figure 10. Line current THD at $T_s=10e-6$ S

Sine wave sources produce three-phase current references with the required peak amplitude, phase angel, and frequency.

Line current ($T_s=25e-6$ S)

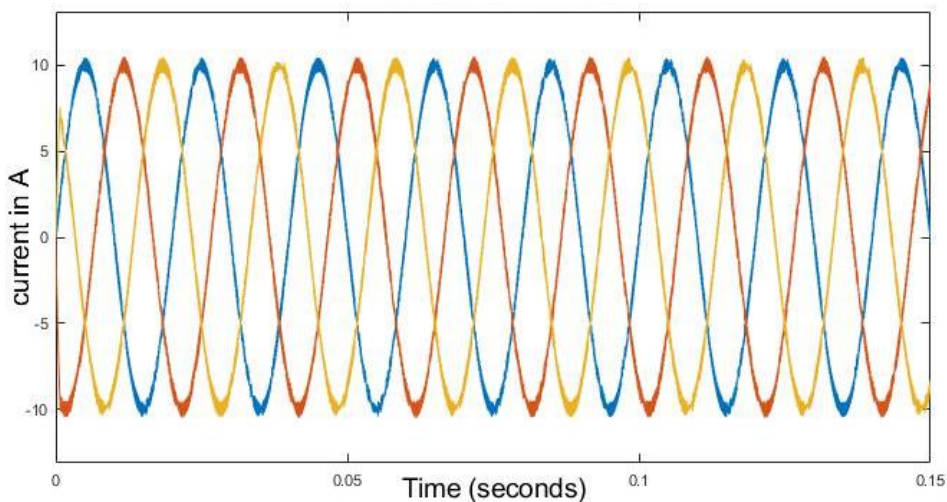


Figure 11. Line current at $T_s=25e-6$ S

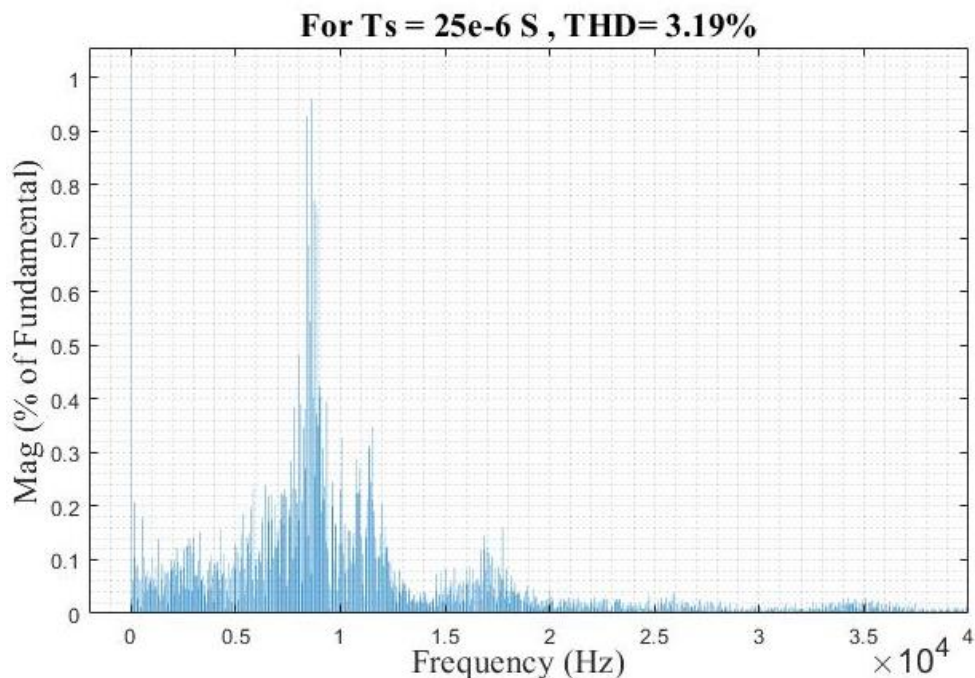


Figure 12. Line current THD at ($T_s=25e-6$ S)

The control can be done in complex coordinates ($\alpha\beta$ coordinates) to minimize the number of predictions. The transformation from one to another must be given, because both

the measured value of load and reference currents are in three phase quantities. This step is not required in few situations where the current reference is in two phase coordinates.

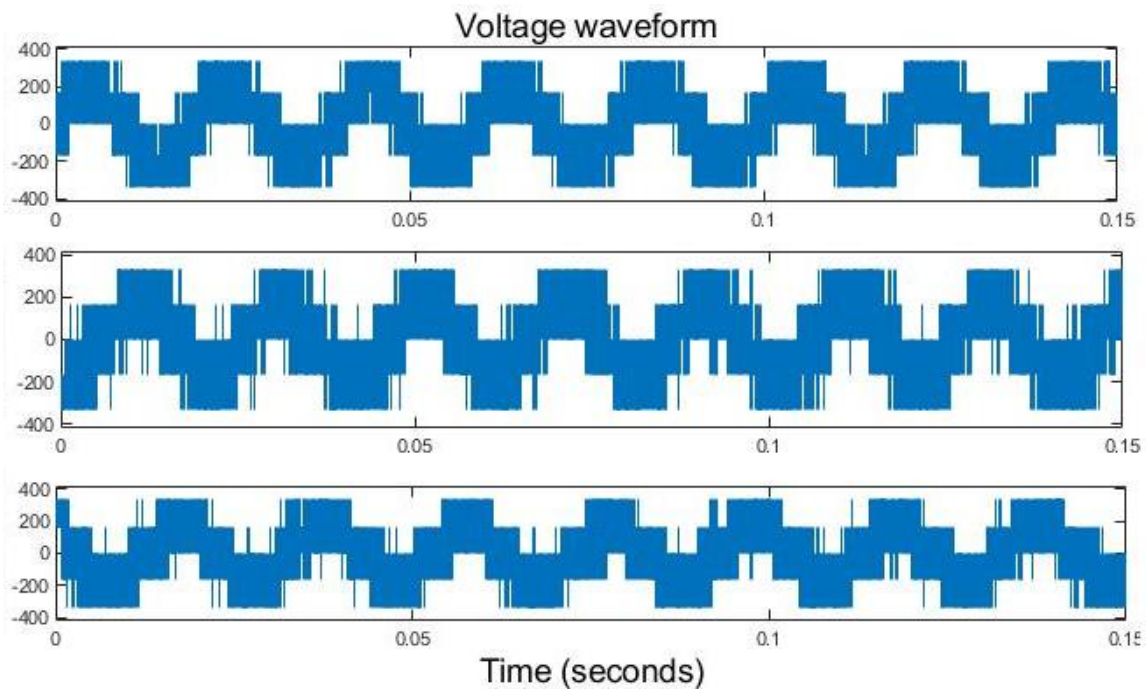


Figure 13. Phase voltage waveform in steady state

The MPC algorithm is employed as an embedded MATLAB S-function, with reference and measured currents given in coordinates as inputs.

4. Conclusion

When compared to a typical PI control system, the suggested approach achieves reduced current error and lower harmonic contents. The performance of PI controllers is determined by how well their parameters are adjusted. There are no parameters to alter in this proposed control approach, but the cost function needs to be defined. The current error can be altered by altering the value of T_s (sampling time). Even though the duty cycle can be modified, it is limited since the inverter's switching state can only be changed once per sample. It performs well in both transient and steady state situations. As a result, the inverter which is connected to the grid could achieve flexibility in power control. Due to the rise of electrification and the ever-increasing demand for high-efficiency electric components, the worldwide megatrend of decarbonization will promote MPC applications in electronics even more. Model-based predictive control (MPC) can be useful in a variety of sectors, including climate control systems (specifically heating, ventilation, and air conditioning applications).

References

- [1] Rodriguez, J. Pontt, J. Silva, C.A. Correa, P. Lezana, P. Cortés, P. Ammann, U. Predictive current control of a voltage source inverter. *IEEE Trans. Ind. Electron.* 2007, 54, 495–503.
- [2] Vazquez, S. Montero, C. Bordons, C. Franquelo, L.G. Design and experimental validation of a model predictive control strategy for a VSI with long prediction horizon. In *Proceedings of the IECON 2013—39th Annual Conference of the IEEE Industrial Electronics Society*, Vienna, Austria, 10–13 November 2013; pp. 5788–5793.
- [3] Acuna, P. Moran, L. Rivera, M. Dixon, J. Rodriguez, J. Improved active power filter performance for renewable power generation systems. *IEEE Trans. Power Electron.* 2013, 29, 687–694
- [4] Shan, Y. Hu, J. Li, Z. Guerrero, J.M. A model predictive control for renewable energy-based ac microgrids without any PID regulators. *IEEE Trans. Power Electron.* 2018, 33, 9122–9126.
- [5] Y. Liu, X. Mao, G. Ning, H. Dan, H. Wang and M. Su, "Model Predictive-Based Voltage Balancing Control for Single-Phase Three-Level Inverters," in *IEEE Transactions on Power Electronics*, vol. 36, no. 11, pp. 12177-12182, Nov. 2021.
- [6] F. Blaabjerg, M. Liserre, and K. Ma, "Power electronics converters for wind turbine systems," *IEEE Trans. Ind. Appl.*, vol. 48, no. 2, pp. 708-719, March/April. 2012.
- [7] M. Malinowski, M. Jasinski and M. P. Kazmierkowski, "Simple direct power control of three-phase PWM rectifier using space-vector modulation (DPC-SVM)," *IEEE Trans. Ind. Electron.*, vol. 51, no. 2, pp. 447-454, April 2004.
- [8] Alemi, P. Bae, C. J. Lee, D. C. (2016). Resonance Suppression Based on PR Control for Single-Phase GridConnected Inverter with LCL filters. *IEEE Journal of Emerging and Selected topic in Power Electronics.*, Vol. 04. No. 2, pp. 459-467.
- [9] Fantino, R. A. Busada, C. A. Solsona, J. A. (2018). Optimum PR Control Applied to LCL Filters with Low Resonance Frequency. *IEEE Trans. Power Electron.*, vol. 33, No. 1, pp. 793–801.
- [10] Mohamed, Y. and Rahman, M. A. Seethapathy, R. (2012). Robust line-voltage sensorless control and synchronization of LCL-filtered distributed generation inverters for high power quality grid connection. *IEEE Trans. Power Electron.*, vol. 27, no. 1, pp. 87–98.

- [11] J. Hu, J. Zhu, G. Platt, and D. G. Dorrell, "Model predictive control of inverters for both islanded and grid-connected operations in renewable power generations," *IET Renew. Power Gener.*, in press.
- [12] J. Rodríguez, J. Pontt, C. A. Silva, P. Correa, P. Lezana, P. Cortés, and U. Ammann, "Predictive current control of a voltage source inverter," *IEEE Trans. Ind. Electron.*, vol. 54, no. 1, pp. 495-503, February 2007.
- [13] M. Preindl, E. Schaltz, and P. Thogersen, "Switching frequency reduction using model predictive direct current control for high- power voltage sources inverters," *IEEE Trans. Ind. Electron.*, vol. 58, no. 7, pp. 2826-2835, 2011.
- [14] J. Scoltock, T. Geyer, and U. Madawala, "Model predictive direct power control for a grid-connected converter with an LCL-filter," in *Proc. IEEE Int. Conf. on Industrial Technology (ICIT)*, 2013, pp. 588-593.
- [15] N. Mohan, T. M. Undeland, and W. P. Robbins, "Power electronics," John Wiley & Sons., USA, 2003.
- [16] W. Kramer, S. Chakraborty, B. Kroposki, and H. Thomas, "Advanced power electronic interfaces for distributed energy systems – part1: systems and Topologies," National Renewable Energy Laboratory, NREL/TP-581-42672, March 2008.
- [17] T. Geyer, "A comparison of control and modulation schemes for medium-voltage drives: Emerging predictive control concepts versus PWM-based schemes," *IEEE Trans. Ind. Appl.*, vol. 47, no. 3, pp. 1380-1389, 2011.
- [18] Y. Zhang, J. Zhu, and W. Xu, "Predictive torque control of permanent magnet synchronous motor drive with reduced switching frequency," in *Proc. IEEE ICEMS Conf.*, 2010, pp. 1–6.
- [19] J. Hu, J. Zhu, G. Platt and D. G. Dorrell, "Model-predictive direct power control of AC/DC converters with one step delay compensation", *Proc. of IEEE 38th Industrial Electronics Society (IECON) Conf.*, pp. 4874–4879, 2012.
- [20] J. Hu, J. Zhu, G. Lei, G. Platt and D. G. Dorrell, "Multi-objective model-predictive control for high power converters," *IEEE Trans. on Energy Convers.*, in press.